

## ORIGINAL ARTICLE

## Heat Transfer Rate Optimisation of Ionanofluid Based Heat Sink Using ANSYS

Balaji Bakthavatchalam<sup>1\*</sup>, Khairul Habib<sup>1</sup>, O.A. Hussein<sup>2</sup>, R. Saidur<sup>3</sup> and Kashif Irshad<sup>4</sup><sup>1</sup>Department of Mechanical Engineering, Universiti Teknologi PETRONAS, 32610 Bandar Seri Iskandar, Perak, Malaysia<sup>2</sup>Department of Mechanical Engineering, College of Engineering, Tikrit University, Tikrit, Iraq<sup>3</sup>Research Centre for Nano-materials and Energy Technology (RCNMET), School of Science and Technology, Sunway University, Malaysia<sup>4</sup>Center of Research Excellence in Renewable Energy, King Fahd University of Petroleum & Minerals, Dhahran, Saudi Arabia

**ABSTRACT** – Heat dissipation of various electrical and electronic devices has been a significant concern in the current years of modernisation. Many researchers proved that a liquid-cooled microchannel heat sink (MCHS) is an effective way of removing high heat load. Due to ionic liquids' unique properties such as negligible volatility, non-flammability, high thermal stability, and ionic conductivity, this liquid is combined with nanofluids to synthesise a new class of potential fluids termed Ionanofluids (ionic liquid-based nanofluids). In this research, a numerical simulation of fluid flow and heat transfer characteristics of MWCNT (Multiwalled Carbon Nanotubes) based Ionanofluids as a coolant in a rectangular-shaped microchannel heat sink is analysed. The Two-step method is used for preparing the studied Ionanofluids consisting of 0.5 wt.% of MWCNT nanoparticles ultra-sonicated with a mixture of propylene glycol and 1-Butyl-3-methylimidazolium chloride ([Bmim][Cl]-ionic liquid) fluids. Copper micro channelled heat sink comprising 1 m channel height, 25  $\mu\text{m}$  of channel diameter, and 0.7 m channel width is modelled and simulated with ANSYS-Fluent. The results showed that the heat transfer coefficient increases about 11.4% while the thermal resistance decreases about 15.18% by using the proposed ionanofluids with the concentration of 0.5 wt.% at  $\text{Re}=2000$  compared with that of an MCHS with propylene glycol. Moreover, the pressure drop along the studied MCHS increased up to a maximum of 30 kPa for higher heat gradients. Ionanofluids decreased the thermal resistance and temperature difference between the heated surface of the MCHS and Ionanofluids inlet to a greater extent when validated with pure base fluid and previous studies. From the simulated results, a better cooling performance is observed with Ionanofluids compared to pure propylene glycol (PG) for the proposed microchannel heat sink.

## ARTICLE HISTORY

Received: 6<sup>th</sup> Aug 2020Revised: 4<sup>th</sup> Nov 2020Accepted: 24<sup>th</sup> Nov 2020

## KEYWORDS

Heat sink;  
Ionanofluid;  
ANSYS;  
Cooling;  
Thermal resistance

## NOMENCLATURE

MCHS	micro channel heat sink	s	surface of the solid
MWCNT	multi-wall carbon nanotubes	T	temperature
ANN	artificial neural network	$\epsilon$	heat dissipation rate
Q	heat transfer rate	p	pressure
[Bmim][Cl]	1-Butyl-3-methylimidazolium chloride	u	velocity in x- axis
PG	propylene glycol	v	velocity in y-axis
TiO <sub>2</sub>	titanium dioxide	W	velocity in z-axis
Al <sub>2</sub> O <sub>3</sub>	aluminium oxide	Q	heat dissipation
Re	Reynolds number	A	area
d	diameter of the channel	$\mu\text{m}$	micrometre
w	width of the heat sink	$\rho$	density
h	height of the heat sink	$\mu$	viscosity
t	thickness	$V_{\text{in}}$	velocity inlet

## INTRODUCTION

Many experiments have been carried out in the past decade to enhance the thermal performance of heats sinks via conventional heat transfer fluids (HTFs). Using nanofluids (a combination of nanoparticles and base fluids) as HTF is considered as a remedy to many heat transfer problems owing to their increased thermophysical properties relative to pure liquids (water and ethylene glycol) [1, 2]. For instance, high efficient thermal performance is reported by Sarafraz et al. [3, 4] using oil-based silver nanofluids and acetone-based zirconia nanofluids relative to pure base fluids. Similarly, many researchers concentrated on exploring the potential of nanofluids with conventional heat transfer fluids like water, synthetic oils and ethylene glycol [5-7]. Nevertheless, authors have not discussed the stability period and maximum

decomposition temperature, which is essential for deciding the target applications. Moreover, water and oil-based nanofluids are not appropriate for medium to high-temperature applications. Besides, the major problems of nanofluids are sedimentation, pressure drop, erosion and fouling, which limit its applications in thermal systems [8-11]. Therefore, for medium to high-temperature applications, it is important to synthesise novel nanofluids based on non-traditional fluids. At present, ionic liquids are one of the new class of fluids that has a wider temperature range ( $\leq 500$  °C) [12]. Mixing ionic liquids and nanoparticles may create a fascinating substance that retains the basic ionic liquid properties and increases thermophysical properties due to the dispersion of nanoparticles. In the same way, incorporation of nanofluids with ionic liquids produces a novel fluid called 'Ionanofluids' which exhibits good thermal stability, high heat capacity and low vapour pressure. These desirable properties render Ionanofluids very attractive for use as heat transfer fluid in medium and high-temperature applications. Hosseinghorbani et al. [13] numerically investigated the heat transfer performance of graphene-based Ionanofluid in a concentrated solar collector. They found a maximum heat transfer enhancement of 7.2% over the base fluid. Chen et al. [14] investigated the effect of SiC Ionanofluid as heat transfer fluid in direct absorption solar collector (DASC). The results revealed that the tested Ionanofluid achieved a maximum extinction coefficient of  $5.8 \text{ cm}^{-1}$  which shows its potential for superior solar material. Unfortunately, only a few works are reported on the application of Ionanofluids that too in solar plants. As such, this study focused on the application of Ionanofluids in Microchannel Heat Sinks (MCHS). Revolutionary challenges have been performed to increase thermal systems' heat dissipation with MCHS by increasing their heat transfer coefficient, surface area, and thermal conductivity of working fluid [15-17]. Amidst different approaches, the most successful way to overcome these challenges in thermal management seems to be innovative Ionanofluids based microchannel heat sinks. With proper design and use of Ionanofluids in microchannel heat sinks, the flow can be precisely distributed between the channels, flow distance can be decreased, and laminar flow can be determined, while high coefficients of heat transfer, high surface to volume ratio, and decreased pressure drops can be achieved. Zargartalebi et al. [18] analysed the effect of nanoparticles on a microchannel heat sink, where they found that the distribution of nanoparticles dominated the temperature profile and the flow geometry in the MCHS. Ho et al. [19] researched  $\text{Al}_2\text{O}_3$ /Water nanofluids efficiency in a Docosane-Layered MCHS with the Reynolds number of 1549 at a greater mass concentration of 8%. They reported that alumina nanofluid increased the heat transfer rate and Nusselt number to a greater extent.

In the latest research, Naphon et al. [20] utilised ANN and CFD techniques with Eulerian two-phase approach to determine nanofluids heat transfer behaviour and pressure drop in an MCHS. They compared their experimental results with the numerical (ANN and CFD) results that showed a maximum error of 1.25% only. By blending  $\text{TiO}_2$  nanoparticles with deionised water, Nakharinr et al. [21] formulated high efficient  $\text{TiO}_2$  nanofluids which increased the convective heat transfer of the MCHS to 18.56% at 0.015 Vol%. Bezaatpour et al. [22] focused on studying the heat transfer characteristics and pressure drop of a Microchannel porous and non-porous heat sinks with magnetite nanofluid, which led to a heat transfer enhancement of 14% and 547% with non-porous and porous media, respectively. Ambreen et al. [23] used a two-phase Eulerian model for analysing the efficiency of a micro pin fin heat sink with alumina nanofluid at different volume fractions (0-1 vol.%). They obtained a maximum heat transfer coefficient enhancement of 16% at a maximum pressure difference of 2760 Pa and 1% volume concentration. Zhao et al. [24] found that CPU temperature can be reduced to a maximum difference of  $5.76^\circ\text{C}$  when compared with water by using rectangularly grooved and cylindrical bugled heat sinks. Many researchers have used nanofluids to improve the heat transfer capacity of a system [25-28]. The addition of ionic liquids can achieve further improvements in the thermophysical properties of nanofluids. Ionic liquid-based nanofluids have recently been regarded as an innovative method of tremendous heat transfer increase by improving the heat transfer fluid's thermal properties. Recently, Paul et al. [29] prepared an Ionanofluid using a 1-butyl-3-methylimidazolium ionic liquid with  $\text{Al}_2\text{O}_3$  nanoparticles to assess the heat transfer efficiency of a circular tube. They observed a significant increase in heat transfer rate coefficient for ionic liquid-based nanofluid. Oster et al. [30] presented the mechanism of heat transfer rate enhancement using Ionanofluids doped with boron nitride and graphite, where graphite induced Ionanofluids resulted in a maximum heat capacity enhancement of 34%. Different scientists have carried out laboratory research to determine Ionanofluid effects in various applications of heat transfer [31-33].

There have been numerous reports on heat transfer studies of conventional coolants such as air, water, petroleum, ethylene glycol, and nanofluids. However, there are only limited researches on the application of Ionanofluids in heat transfer devices. Therefore, this paper aims to present the influence of a new ionic liquid-based nanofluid in a heat sink with the microchannel. In order to analyse the fluid flow and convective heat transfer properties of the prepared MWCNT/PG/BmimCl (Ionanofluid) coolant in a copper MCHS, a 3-dimensional CFD model is developed with the commercial FLUENT software package. The variations of the heat transfer coefficient, thermal resistance and pressure drop of the MCHS are discussed with the synthesised Ionanofluid and compared to pure base fluid (propylene glycol).

## MATERIALS AND METHODS

### Materials and Chemicals

[BMIM][Cl], purchased from Sigma Aldrich, USA, was selected as a part of the base fluid due to its thermal stability of more than  $350$  °C. MWCNT nanoparticles with an average length of 13 nm to 20 nm and 10 nm diameter were procured from the same company. The raw image of the studied MWCNT nanoparticles is shown in Figure 1(a). Moreover, the propylene glycol solution was also bought from Sigma Aldrich. The morphology of the MWCNT nanoparticles is analysed using the FESEM images displayed in Figure 1(b). Defects in carbon nanotubes result in low-temperature

oxidation, and therefore defect analysis has proved to be an excellent technique to enhance the oxidative stability of materials [34-36]. As such, the procured nanoparticles should be free from large defects. In accordance with the FESEM image, the presence of wrinkled walls, irregular nano lobes, kinks and some sidewall breakages revealed the defect formations. More detailed analysis of the studied MWCNT nanoparticles was recorded in our previous literature [37].

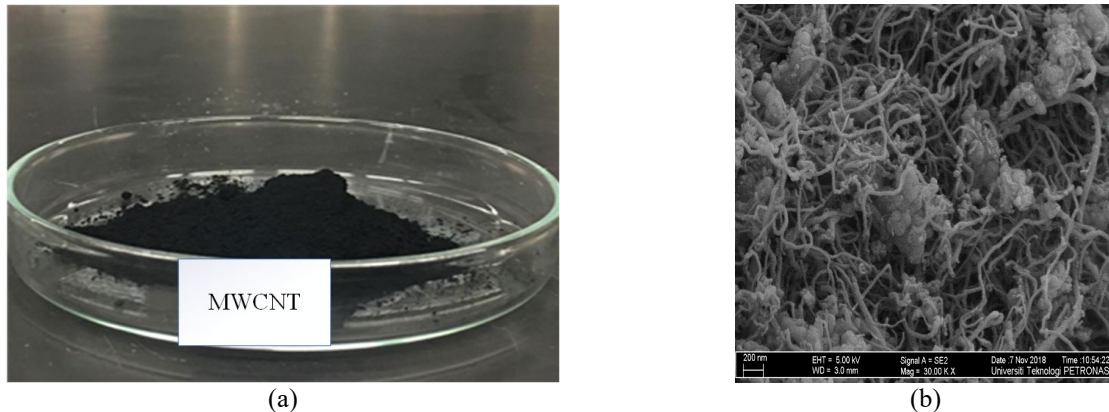


**Figure 1.** (a) Photograph of MWCNT nanoparticle (b) FESEM image of MWCNT nanoparticle at different magnitude.

### Preparation of Ionanofluid

The two-step method was used to prepare the proposed Ionanofluids. In a mixture of propylene glycol and BmimCl (50:50), 0.5 wt% of MWCNT nanoparticles were added, followed by a magnetic agitation (HTS 1003 Hotplate Stirrer, LABMART) of 30 minutes. The magnetic stirring helps the nanoparticles to be mixed well with the base fluids. The suspensions obtained were dispersed thoroughly for 2 hours by a 750 W, 50 kHz ultrasonic device (Ultrasonics VCX-750 Vibra cell) where the nanoparticle is broken down into tiny pieces to enhance the dispersion stability. The obtained Ionanofluids was stable for about one week without any aggregation.

### Instruments

Morphological characteristics of the studied MWCNT nanoparticles is determined by Zeiss Supra 55 VP FESEM equipment. FESEM can be used to characterise the samples down to a resolution of 1 to 4 nm with an accelerating voltage of 100 V to 30 kV. By observing spontaneous fluctuations of light intensity from a suspension, particle size may be determined. Here, the particle size distribution and zeta potential of MWCNT nanoparticles in the dispersed base fluid is analysed using Anton Paar Litesizer 500 which is mainly dependent on the theory of Brownian Motion and surface charge of the nanoparticles. The thermal conductivity of the studied samples is measured by KD2 Pro thermal conductivity meter (Decagon devices, USA) whereas the density of the sample is measured by a Densitymeter (Anton Paar, DMA 1001). Furthermore, the viscosity and specific heat capacity of the tested samples are evaluated using Rheometer (Anton Paar, MCR92) and Differential Scanning Calorimetry (Linseis DSC 1000/°C), respectively.

### CFD Procedure

Following methodologies were adopted to perform computational fluid dynamics simulation of MCHS.

#### Modelling of MCHS

The MCHS geometry is drawn in commercial ANSYS software as shown in Figure 2 with external dimensions of 25  $\mu\text{m}$   $\times$  1000 mm  $\times$  700 mm (t  $\times$  h  $\times$  w) and 25  $\mu\text{m}$  of channel diameter. The proposed micro channel-based heat sink consists of rectangular prism-shaped sections in which the working fluid flows.

#### Generation of mesh

A discretisation of the designed three-dimensional (3D) model of the micro channel-based heat sink was done after generating the model in ANSYS, which is shown in Figure 3. The mesh contained tetra elements, and a mesh size of 0.3 mm was applied to the model. To validate the mesh size in steady-state, mesh convergence analysis was carried out with various elements counting from 1 million to 5 million. Meanwhile, the mesh model consists of 87,036 elements and 3,48,144 nodes. The generated mesh had an average skewness of 0.5, the cell aspect ratio of 1, average orthogonality of 0.8 and an average quality element of 0.93. The integrated meshes of the tube (microchannel) and the heat sink is depicted in Figure 3(a). The zoomed view of the squared mesh is presented in Figure 3(b). The full mesh of the whole MCHS is shown in Figure 3(c). These high-quality mesh images confirm that the right mesh design requirements, grid-independent approach and essential geometric details are well endorsed.

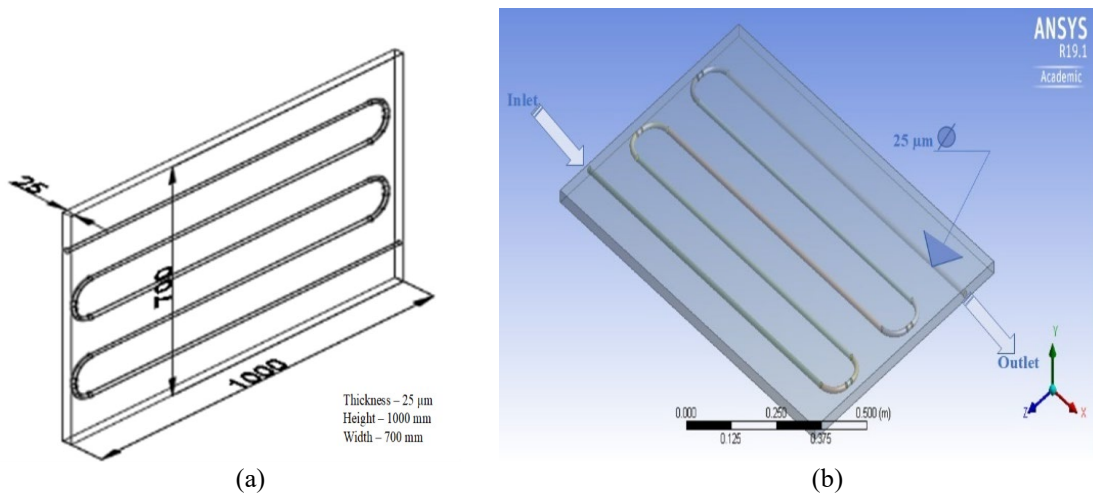


**Figure 2.** (a) Geometric model of the MCHS with external dimensions (b) CFD model of the MCHS with internal dimensions.

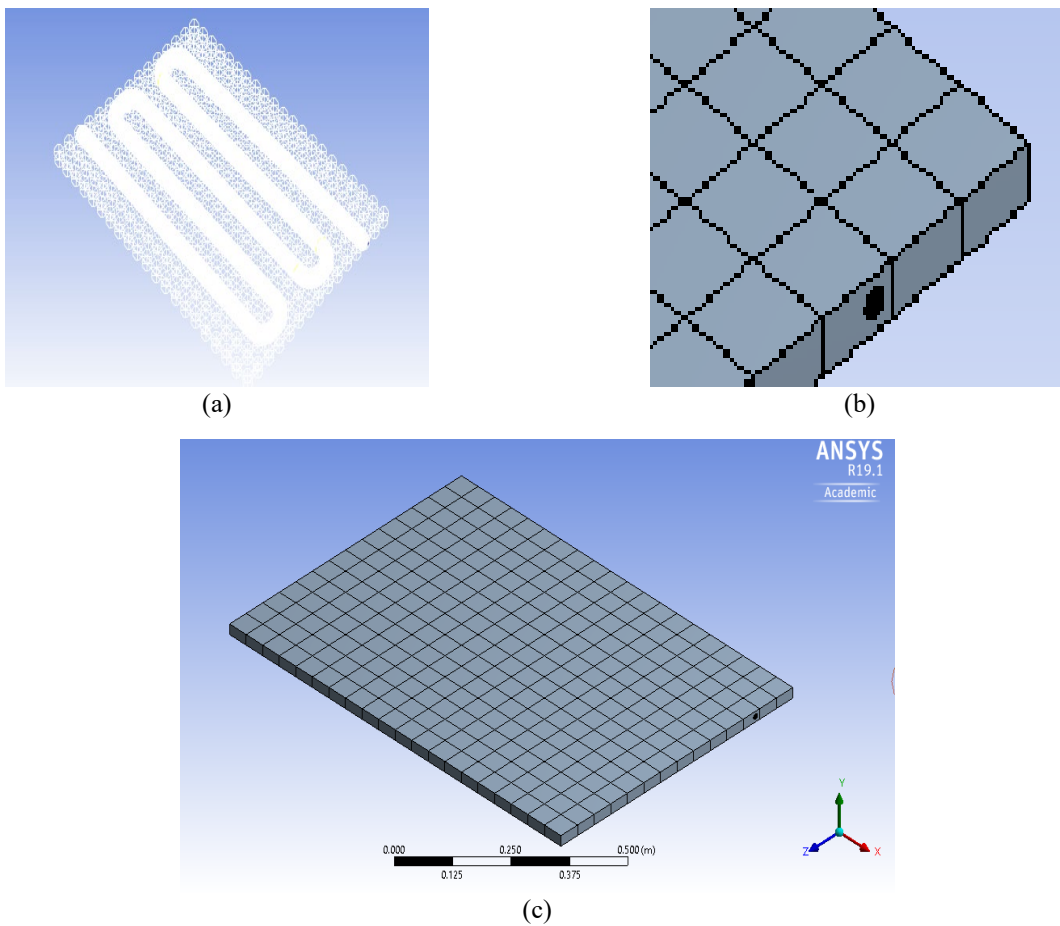


**Figure 3.** (a) Tube and heat sink mesh, (b) zoomed image of meshed MCHS and (c) total body mesh.

*Material properties*

Table 1 shows different thermophysical properties of the proposed CFD associated materials (base fluids and nanoparticles) of the rectangular-shaped microchannel heat sink.

**Table 1.** Thermophysical properties of the materials at 303 K.

Materials	Thermal conductivity (W/m.K)	Density (kg/m <sup>3</sup> )	Viscosity (Pa.S)	Specific heat capacity (kJ/kg.K)
MWCNT	3000	2100	-	1.10
[Bmim][Cl]	0.576	1230	0.7	0.49
Propylene Glycol	0.187	1036	0.042	3.34
MWCNT+[BMIM][Cl]+PG	0.915	1700	0.8	1.53

### Physical modelling

A simple conventional MCHS is chosen in this study to avoid complex configurations. Moreover, a complex structure could result in more thermal resistance and less flow rate of coolant. The proposed system consists of a microchannel with a single inlet and outlet, see Figure 3(b). This MCHS have a width of 700m and a depth of 1000 mm with 25  $\mu\text{m}$  hydraulic diameter channel. It is covered by rectangular metal surfaces (copper) as used in conventional microchannel heat sinks. The microchannel is curved in a way to facilitate the uniform flow of the coolant. Different physical models were used to perform CFD simulation of a rectangular microchannel heat sink using Ionanofluids as working fluid, which is shown below. The equations used in this model are presented from Eq. (1) to Eq. (9).

i. Flow behaviour

This study intends to test the behaviour of the fluid in both the laminar and turbulent regime, and therefore the turbulent model was preferred to simulate the mean flow characteristics. As such, the K-epsilon turbulent modelling technique is used for CFD simulation where K is the kinetic energy and epsilon is the heat dissipation.

ii. Energy system modelling

In the ANSYS software, the energy model is turned on to study the temperature of the heat sink where the working fluid temperature and heat flux at the required surface can be identified.

iii. Governing equation and boundary condition

In this study, Navier-stokes and continuity equations are chosen to carry out the numerical simulation on the effect of Ionanofluids on the performance of the MCHS. This equation is based on Newton's second law of motion and thus, governs fluid movement. Navier stokes equation indicates the conservation of momentum, whereas the continuity equation illustrates the conservation of mass. By using these equations, the fluid speed and its pressure can be predicted in a given geometry.

The governing equations for Ionanofluid flow are resolved using the finite volume method. In terms of continuity, momentum and energy equations, the following assumptions are considered.

- fluid flow and heat transfer are 3-dimensional, laminar, and steady
- the fluid is considered as incompressible and single phase
- both fluid and heat sinks assumed to be temperature independent
- gravity force and heat transfer from the radiation are insignificant

Continuity equation,

$$\frac{\partial u}{\partial x} + \frac{\partial v}{\partial y} + \frac{\partial w}{\partial z} = 0 \quad (1)$$

X-momentum equation:

$$\rho_f \left( u \frac{\partial u}{\partial x} + v \frac{\partial u}{\partial y} + w \frac{\partial u}{\partial z} \right) = -\frac{\partial p}{\partial x} + \mu_f \left( \frac{\partial^2 u}{\partial x^2} + \frac{\partial^2 u}{\partial y^2} + \frac{\partial^2 u}{\partial z^2} \right) \quad (2)$$

Y-momentum equation:

$$\rho_f \left( u \frac{\partial v}{\partial x} + v \frac{\partial v}{\partial y} + w \frac{\partial v}{\partial z} \right) = -\frac{\partial p}{\partial y} + \mu_f \left( \frac{\partial^2 v}{\partial x^2} + \frac{\partial^2 v}{\partial y^2} + \frac{\partial^2 v}{\partial z^2} \right) \quad (3)$$

Z-momentum equation:

$$\rho_f \left( u \frac{\partial w}{\partial x} + v \frac{\partial w}{\partial y} + w \frac{\partial w}{\partial z} \right) = -\frac{\partial p}{\partial z} + \mu_f \left( \frac{\partial^2 w}{\partial x^2} + \frac{\partial^2 w}{\partial y^2} + \frac{\partial^2 w}{\partial z^2} \right) \quad (4)$$

Energy equation for the fluid:

$$\rho_f c_{pf} \left( u \frac{\partial T_f}{\partial x} + v \frac{\partial T_f}{\partial y} + w \frac{\partial T_f}{\partial z} \right) = k_f \left( \frac{\partial^2 T_f}{\partial x^2} + \frac{\partial^2 T_f}{\partial y^2} + \frac{\partial^2 T_f}{\partial z^2} \right) \quad (5)$$

Energy equation for the solid wall:

$$k_s \left( \frac{\partial^2 T_s}{\partial x^2} + \frac{\partial^2 T_s}{\partial y^2} + \frac{\partial^2 T_{fs}}{\partial z^2} \right) = 0 \quad (6)$$

Local convection heat transfer coefficient along the tube is given by:

$$h = \frac{Q}{A(T_w - T_m)} \quad (7)$$

where  $T_m$  and  $T_w$  are mean fluid temperature and wall temperature, respectively

The Reynolds number is defined as:

$$Re = \frac{\rho UD}{\mu} \quad (8)$$

The pressure drop can be calculated as follows:

$$\Delta p = f \left( \frac{L}{D_h} \right) \left( \frac{\rho u^2}{2} \right) \quad (9)$$

where  $f$  is the friction factor, and  $D_h$  is the hydraulic diameter

### Boundary conditions

The schematic structure of the studied rectangular MCHS with boundary condition is shown in Figure 4. The Ionanofluids enter the tube at a uniform speed and temperature, with the same velocity assumed for both the base fluid and particles. The continuous 1500 W heat stream is applied to the bottom of this heat sink and is supposed to be adiabatic on all other surfaces.

i. Boundary conditions at the tube inlet

$$v = v_{in}, \quad u = w = 0 \quad (10)$$

$$T = 303 \text{ K} = T_{in} \quad (11)$$

$$k_{in} = 0.915 \text{ W/m}^2 \quad (12)$$

ii. Boundary condition at the wall. The wall is assumed to be adiabatic:

$$v = u = w = 0, \quad \frac{\partial T_s}{\partial n} = 0 \quad (13)$$

iii. Heat flux boundary:

$$q'' = \frac{Q}{A} = 0.714 \quad (14)$$

iv. Boundary condition at the outlet:

$$p = p_{atm} = 101.325 \text{ kPa} \quad (15)$$

$$\frac{\partial k}{\partial z} = \frac{\partial \varepsilon}{\partial z} = \frac{\partial T_s}{\partial n} = 0 \quad (16)$$

At the exit, the pressure is assumed to be atmospheric pressure. The discretisation of the governing equations in the fluid and solid regions is solved by the method of finite volume. The solution uses a simple algorithm which is based on the pressure correction method. The second-order upwind differentiation scheme is used for energy and momentum equations. The assumptions proposed in this model is depicted in Table 2.

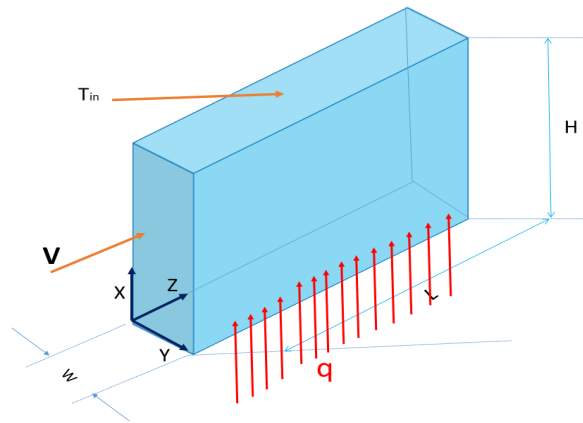


**Figure 4.** External layout of the proposed MCHS.

**Table 2.** Assumptions of the modelled MCHS.

Properties	Assumptions
Microchannel	Heat transfer is constant
Velocity (at inlet)	1 m/s
Pressure (at outlet)	0 Pa
Flow	Turbulent, incompressible, single phase
Wall	No slip ( $u=v=w=0$ )
Fluid Material	MWCNT+[BMIM][Cl]+PG
Body force	Negligible

## RESULTS AND DISCUSSION

The phenomena of Ionanofluids cooling in the proposed heat sink have been studied in this research. Copper heat sink with cylindrical microchannel was selected to make the flow of [Bmim][Cl] ionic liquid and propylene glycol mixture with 0.5 wt.% MWCNT nanoparticles throughout the heat sink. The main objective of this work is to analyse and evaluate the microchannel heat sink characteristics and compare the performance of two different fluids. All two fluids were analysed by simulated results for heat transfer coefficient, thermal resistance, and pressure variations, and compared with Ghasemi et al. [38].

### Particle Size Distribution and Dispersion Stability

Dynamic Light Scattering (DLS) is a technique to characterise the particle size of nanoparticles in nanofluids via scattered light. Especially to determine the influence of the nanoparticles in particle agglomeration, DLS method is performed. Figure 5 presents the variation of particle size as a function of light intensity. From the FESEM image, the diameter of the studied MWCNT nanoparticles ranged from 10 nm to 20 nm. However, the diameter of the nanoparticles obtained in the DLS experiment is very high due to the consequence of aggregation in the as-prepared sample. Agglomeration is a process induced by the surface charge and thickness of the electrical double layer which attributes to the decrease of electrostatic repulsive forces. The uniformity of the particle size distribution is described in terms of the Polydispersity Index (PDI). In order to maintain an excellent dispersion of particles in base fluids, the PDI value should be less than 10%. The as-prepared samples obtained a PDI value of 27% that attributes to the moderate colloidal stability, and this is consistent with the previous study [39].

Stability of the prepared nanofluid is examined through zeta potential method and visual inspection method. The as-prepared sample showed an average zeta potential value of -30 mv that can be considered as moderate stability. Furthermore, the rate of agglomeration or clustering is examined with the naked eye through the visual inspection method. The dispersion stability (agglomeration) of nanofluids usually depends on the preparation technique, temperature, ultrasonication time, base fluid type and nanomaterials. In this study, the visual inspection analysis is conducted for seven days. Based on the images, there was not any significant sedimentation or clustering observed for the first week. But a transparent colour was observed from Day 5, which shows the impact of agglomeration.

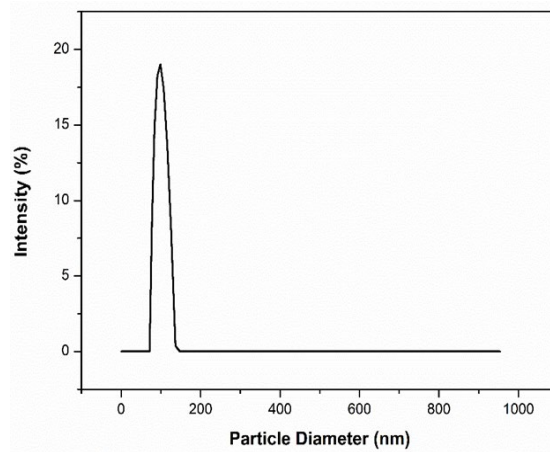


**Figure 5.** Particle size distribution of MWCNT nanoparticles dispersed in the base fluid.

### Solution Calculation

The default ANSYS FLUENT parameters are usually acceptable, and a single click is essential for the generated mesh to start the simulation. From the simulated results, it is found that the obtained solution regularly converged with respect to time. Other than the continuity residual, the remaining residuals (velocity, energy) have converged properly, that are well below the accepted convergence tolerance level. Moreover, the continuity tolerance level was around  $1e-01$ , which was very close to other residual tolerance values of  $1e-04$ , confirming the effective convergence of the solution.

### Thermal Analysis

An effective heat sink requires less thermal resistance and high-temperature difference for enhanced efficiency. The modelled heat sink with different dimensions is subjected to steady-state thermal analysis. Figure 6 displays the temperature of the simulated heat sink. The figure demonstrates that the temperature of the MCHS dropped to 302 K ( $3.022e+02$  K), which can be attributed to the effect of Ionanofluids used in the heat sink. This illustrates that Ionanofluids significantly decreased the temperature of the studied heat sink. These outcomes indicate that an improvement of nanofluids' thermophysical properties with ionic fluids may enhance the efficiency of heat transfer in MCHS. Moreover, the addition of MWCNT nanoparticles with the base fluid at 0.5 wt.% concentration persuaded a temperature decrease in the MCHS base, which is depicted in blue colour.

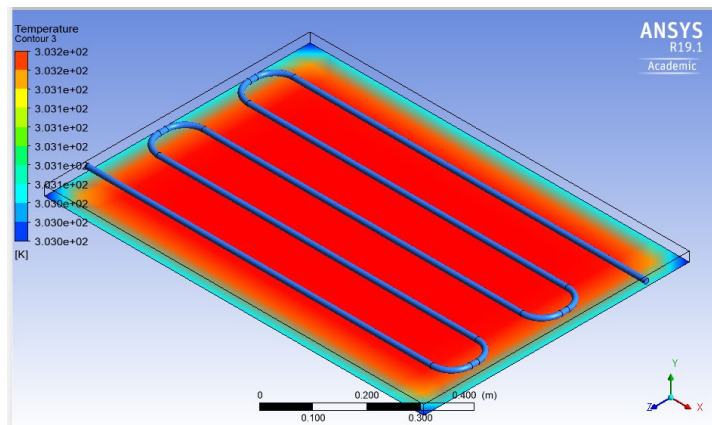


**Figure 6.** Thermal analysis of the studied heat sink.

### Heat Transfer Coefficient

Heat transfer coefficient facilitates the transfer of heat from a boundary surface to a fluid stream in a convective process. Figure 7 displays the change in the coefficient of heat transfer for three fluids with respect to Reynolds number variation. As indicated in the graph, the heat transfer coefficient difference is smaller for the studied Ionanofluids when compared with pure propylene glycol and  $\text{TiO}_2/\text{water}$  nanofluid for the given Reynolds number. Furthermore, only a slight difference was observed for the as-prepared Ionanofluids and  $\text{TiO}_2/\text{water}$  nanofluids. However, all the studied fluids followed the same trend of increase in HTC with an increase in the Reynolds number. Compared to the as-prepared Ionanofluid,  $\text{TiO}_2/\text{water}$  nanofluid revealed a maximum HTC of  $2100 \text{ W/m}^2\text{K}$ . Also, the obtained results illustrated that the optimum HTC for the examined Ionanofluid and propylene glycol was  $2031 \text{ W/m}^2\text{K}$  and  $1823 \text{ W/m}^2\text{K}$ , respectively, under the tested conditions. These findings prove that the addition of ionic liquid in the MWCNT/PG nanofluid has dramatically enhanced HTC. This increase in the HTC of the Ionanofluid may be attributed to the anion-cation interactions

induced by the [Bmim][Cl] ionic liquid. Consequently, these results demonstrate that the proposed Ionanofluids retained more heat energy than the other tested fluids.

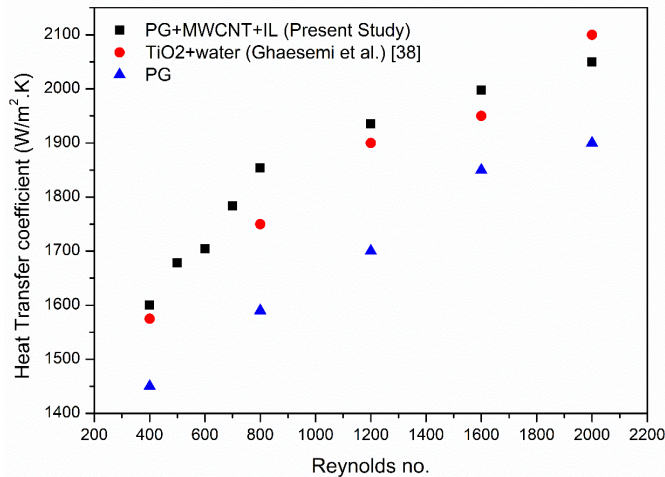


**Figure 7.** Heat transfer coefficient of the MCHS with different fluids at 0.5 wt.%.

### Thermal Resistance

Thermal resistance is defined as the total temperature drop across the system to that of the real heat flow rate that mainly depends on the temperature of the coolant and heat sink wall. It plays a significant role in increasing the effectiveness of the MCHS. Figure 8 represents the variation of thermal resistance with certain Reynolds number for propylene glycol, TiO<sub>2</sub>/water nanofluid, and the synthesised Ionanofluids. In general, the increase in Reynolds number provides an increased heat transfer rate and also reduces the maximum and average thermal resistance. As illustrated by the graph, thermal resistance decreases with increasing Reynolds number. The results demonstrate that all the studied samples are quite susceptible to Reynolds number, with PG/MWCNT/IL the most and pure propylene glycol the least one. This confirms that the dispersion of ionic liquids in nanofluids results in the decrease of thermal resistance. It can be seen that when the Reynolds number increases, the thermal resistance decreases, which coincides with the previous study [19]. This is due to the increasing inlet speed that increased the Brownian motion. Thus, the Ionanofluids thermal transport is enhanced, which causes the coefficient of convective heat transfer to increase and thermal resistance to decrease at high Reynolds number.

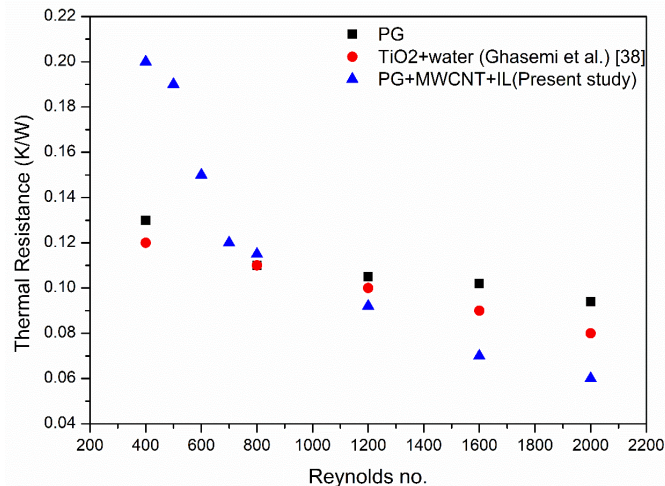


**Figure 8.** Thermal resistance of MCHS with different fluids at 0.5 wt.%.

### Pressure Drop

An essential aspect of the fluid system is pressure drop which plays a significant role in achieving the desired pumping power to maintain the uniform circulation of working fluid. It is characterised as the difference of total pressure in a fluid transmission system between two points which is mainly caused by frictional forces. Figure 9 shows the relationship between the pressure drop and the Reynolds number among propylene glycol, TiO<sub>2</sub>/water nanofluids, and Ionanofluids where the ionic liquid-based nanofluid showed lesser pressure drop of 30 kPa while TiO<sub>2</sub>/water nanofluid and PG revealed 50 kPa and 42 kPa, respectively at 2000 Re. All the three fluids increased the pressure drop with increase in Reynolds number that may be due to their higher viscosity that causes the liquid to be moved by higher pressure that was consistent with this study till 1000 Re. The results proved that the as-prepared Ionanofluid had not followed the viscosity relation

above 1000 Re as discussed earlier. Due to the small microchannel gaps, the fluid acceleration increased, leading to high frictional resistance and pressure loss that may increase the pressure drop of the fluid, which is revealed in the graph. The graph demonstrates the variation of numerically predicted pressure drop with Reynolds number for three studied fluids. The pressure increased from 4 kPa to 50 kPa, consistent with standard microchannel heat sinks that can help reduce the danger of leakages.

Furthermore, this value increases monotonically with respect to the Reynolds number increase, which was also observed in previous literature [40, 41]. The phenomena behind the pressure difference are due to the fact that when the velocity of the fluid rises, the shear stress on the microchannel increases attributing to a higher pressure drop. Besides, the obtained values are also compared with an experimental study conducted by Qu et al. [42] which shows that the pressure drop increases with a significant rate as a function of Reynolds number but follows the same trend of the other fluids.

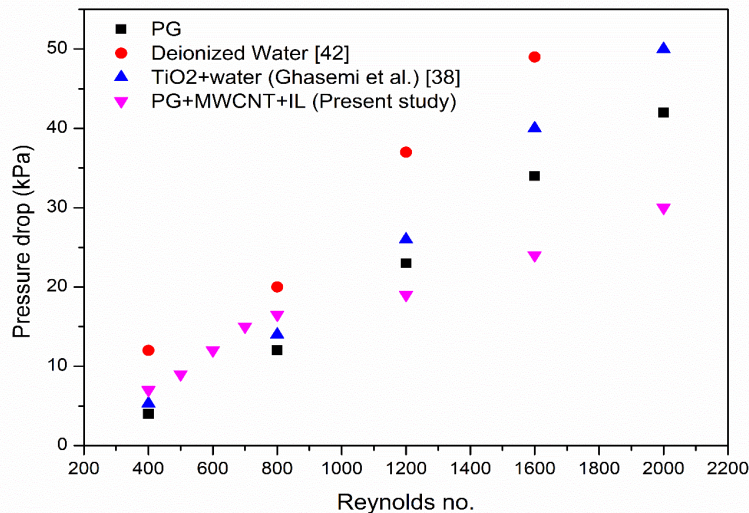


Figure 9. Pressure drop of MCHS with different fluids at 0.5 wt.%.

## CONCLUSION

Ionanofluids containing multi-walled carbon nanotubes dissolved in propylene glycol and [Bmim][Cl] ionic liquid with a mass fraction of 0.5 wt% were prepared, and its thermal performance was analysed in a microchannel heat sink via ANSYS and compared with previous literature. Temperature-dependent thermophysical properties of the prepared samples were taken into account for the simulation. The microchannel heat sink was simulated with 1500 W of heat flux and in laminar flow conditions. This research is performed to model and simulate a heat sink cooled by Ionanofluids, to improve heat transfer with the as-prepared Ionanofluids. ANSYS software was used to simulate the heat sink flow that proved the potential of the studied Ionanofluid as an alternative working fluid for thermal applications. Thermal properties of pure base fluid (propylene glycol) and nanofluid (TiO<sub>2</sub>/water) were compared and validated with the prepared Ionanofluid (MWCNT + propylene glycol + BmimCl). Indeed, the application of Ionanofluids with 0.5 wt.% concentration improved heat transfer coefficient by 11.4% and decreased the thermal resistance up to 15.18%. Compared to the other two fluids, Ionanofluids resulted in higher heat transfer characteristics in the simulated microchannel heat sink at higher Reynolds number. Meanwhile, the thermal resistance and pressure drop of the tested Ionanofluids followed the same trend of the previous study with slight fluctuations in their values. The future directions are as follows.

- i. Since ionic liquids are recyclable, thermally stable and eco-friendly, the study of different ionic liquids with different nanofluids is needed.
- ii. Develop an appropriate model to study the effects of Ionanofluids in thermal system simulations.
- iii. Only limited efforts are dedicated to investigating the effect of agglomeration or dispersion stability on nanofluid based heat sinks performance.

## ACKNOWLEDGEMENT

The authors appreciate Universiti Teknologi PETRONAS for laboratory facilities and financial assistance under YUTP grant no. 015LC0-118.

## REFERENCES

- [1] Azmi W, Zainon S, Hamid K, Mamat R. A review on thermo-physical properties and heat transfer applications of single and hybrid metal oxide nanofluids. *Journal of Mechanical Engineering and Sciences* 2019;13:5182 - 211.

- [2] Oumer AN, James LTC, Azizuddin AA. A review on thermo-physical properties of bio, non-bio and hybrid nanofluids. *Journal of Mechanical Engineering and Sciences* 2019;13: 5875-904.
- [3] Sarafraz MM, Arya A, Nikkiah V, Hormozi F. Thermal performance and viscosity of biologically produced silver/coconut oil nanofluids. *Chemical and Biochemical Engineering Quarterly* 2016;30:489.
- [4] Sarafraz MM, Pourmehran O, Yang B, Arjomandi M. Assessment of the thermal performance of a thermosyphon heat pipe using zirconia-acetone nanofluids. *Renewable Energy* 2019;136:884-95.
- [5] Singh T, Almanassra I, Olabi A, Al-Ansari T, McKay G, Muataz AA. Performance investigation of multi-wall carbon nanotubes based water/oil nanofluids for high pressure and high temperature solar thermal technologies for sustainable energy systems. *Energy Conversion and Management* 2020;225:113453.
- [6] Sarafraz MM, Safaei MR, Tian Z, Goodarzi M, Bandarra Filho EP, Arjomandi M. Thermal assessment of nano-particulate graphene-water/ethylene glycol (WEG 60:40) nano-suspension in a compact heat exchanger. *Energies* 2019;12 (10): 1929.
- [7] Sarafraz M, Arya H, Saedi M, Ahmadi D. Flow boiling heat transfer to MgO-therminol 66 heat transfer fluid: Experimental assessment and correlation development. *Applied Thermal Engineering* 2018;138:552-62.
- [8] Chakraborty S, Panigrahi PK. Stability of nanofluid: A review. *Applied Thermal Engineering* 2020;174:115259.
- [9] Sarafraz MM, Yang B, Pourmehran O, Arjomandi M, Ghomashchi R. Fluid and heat transfer characteristics of aqueous graphene nanoplatelet (GNP) nanofluid in a microchannel. *International Communications in Heat and Mass Transfer* 2019;107:24-33.
- [10] Sangmesh B, Gopalakrishna K, Manjunath SH, Kathyayini N, Kadirgama K, Samykano M, et al. Experimental investigation on HSFP using MWCNT based nanofluids for high power light emitting diodes. *Journal of Mechanical Engineering and Sciences* 2018;12:3852-65.
- [11] Safiei W, Rahman M, Yusoff A, Radin M. Preparation, stability and wettability of nanofluid: A review. *Journal of Mechanical Engineering and Sciences* 2020;14:7244-57.
- [12] Cao Y, Mu T. Comprehensive investigation on the thermal stability of 66 ionic liquids by thermogravimetric analysis. *Industrial & Engineering Chemistry Research* 2014;53:8651-64.
- [13] Hosseinghorbani A, Mozaffarian M, Pazuki G. Application of graphene oxide Ionanofluid as a superior heat transfer fluid in concentrated solar power plants. *International Communications in Heat and Mass Transfer* 2020;111:104450.
- [14] Chen W, Zou C, Li X. An investigation into the thermophysical and optical properties of SiC/ionic liquid nanofluid for direct absorption solar collector. *Solar Energy Materials and Solar Cells* 2017;163:157-63.
- [15] Dahiya A, Amer M, Sajjad U, Borah P, Sehgal SS, Singh H. An experimental study on microchannel heat sink via different manifold arrangements. *SN Applied Sciences* 2019;2:40.
- [16] Tlau L, Ontela S. Entropy generation in MHD nanofluid flow with heat source/sink. *SN Applied Sciences* 2019;1:1672.
- [17] Kahalerras H, Fersadou B, Nessab W. Mixed convection heat transfer and entropy generation analysis of copper-water nanofluid in a vertical channel with non-uniform heating. *SN Applied Sciences* 2019;2:76.
- [18] Zargartalebi M, Azaiez J. Heat transfer analysis of nanofluid based microchannel heat sink. *International Journal of Heat and Mass Transfer* 2018;127:1233-42.
- [19] Ho CJ, Liao J-C, Li C-H, Yan W-M, Amani M. Experimental study of cooling performance of water-based alumina nanofluid in a minichannel heat sink with MEPCM layer embedded in its ceiling. *International Communications in Heat and Mass Transfer* 2019;103:1-6.
- [20] Naphon P, Wiriyaart S, Arisariyawong T, Nakharintr L. ANN, numerical and experimental analysis on the jet impingement nanofluids flow and heat transfer characteristics in the micro-channel heat sink. *International Journal of Heat and Mass Transfer* 2019;131:329-40.
- [21] Naphon P, Nakharintr L, Wiriyaart S. Continuous nanofluids jet impingement heat transfer and flow in a micro-channel heat sink. *International Journal of Heat and Mass Transfer* 2018;126:924-32.
- [22] Bezaatpour M, Goharkhah M. Three dimensional simulation of hydrodynamic and heat transfer behavior of magnetite nanofluid flow in circular and rectangular channel heat sinks filled with porous media. *Powder Technology* 2019;344:68-78.
- [23] Ambreen T, Saleem A, Park CW. Numerical analysis of the heat transfer and fluid flow characteristics of a nanofluid-cooled micropin-fin heat sink using the Eulerian-Lagrangian approach. *Powder Technology* 2019;345:509-20.
- [24] Zhao N, Guo L, Qi C, Chen T, Cui X. Experimental study on thermo-hydraulic performance of nanofluids in CPU heat sink with rectangular grooves and cylindrical bugles based on exergy efficiency. *Energy Conversion and Management* 2019;181:235-46.
- [25] Peyghambarzadeh SM, Hashemabadi SH, Hoseini SM, Seifi Jamnani M. Experimental study of heat transfer enhancement using water/ethylene glycol based nanofluids as a new coolant for car radiators. *International Communications in Heat and Mass Transfer* 2011;38:1283-90.
- [26] Ali HM, Ali H, Liaquat H, Bin Maqsood HT, Nadir MA. Experimental investigation of convective heat transfer augmentation for car radiator using ZnO-water nanofluids. *Energy* 2015;84:317-24.
- [27] İlhan B, Ertürk H. Experimental characterization of laminar forced convection of hBN-water nanofluid in circular pipe. *International Journal of Heat and Mass Transfer* 2017;111:500-7.
- [28] Khedkar RS, Sonawane SS, Wasewar KL. Heat transfer study on concentric tube heat exchanger using TiO<sub>2</sub>-water based nanofluid. *International Communications in Heat and Mass Transfer* 2014;57:163-9.

- [29] Paul TC, Mahamud R, Khan JA. Multiphase modeling approach for ionic liquids (ILs) based nanofluids: Improving the performance of heat transfer fluids (HTFs). *Applied Thermal Engineering* 2019;149:165-72.
- [30] Oster K, Hardacre C, Jacquemin J, Ribeiro APC, Elsinawi A. Understanding the heat capacity enhancement in ionic liquid-based nanofluids (ionanofluids). *Journal of Molecular Liquids* 2018;253:326-39.
- [31] Minea AA, Murshed SMS. A review on development of ionic liquid based nanofluids and their heat transfer behavior. *Renewable and Sustainable Energy Reviews* 2018;91:584-99.
- [32] Minea A-A, El-Maghlany WM. Natural convection heat transfer utilizing ionic nanofluids with temperature-dependent thermophysical properties. *Chemical Engineering Science* 2017;174:13-24.
- [33] Bakthavatchalam B, Habib K, Saidur R, Saha BB, Irshad K. Comprehensive study on nanofluid and ionanofluid for heat transfer enhancement: A review on current and future perspective. *Journal of Molecular Liquids* 2020;305:112787.
- [34] Pham CV, Repp S, Thomann R, Krueger M, Weber S, Erdem E. Charge transfer and surface defect healing within ZnO nanoparticle decorated graphene hybrid materials. *Nanoscale* 2016;8:9682-7.
- [35] Pham CV, Krueger M, Eck M, Weber S, Erdem E. Comparative electron paramagnetic resonance investigation of reduced graphene oxide and carbon nanotubes with different chemical functionalities for quantum dot attachment. *Applied Physics Letters* 2014;104:132102.
- [36] Erdem E, Mass V, Gembus A, Schulz A, Liebau-Kunzmann V, Fasel C, et al. Defect structure in lithium-doped polymer-derived SiCN ceramics characterized by Raman and electron paramagnetic resonance spectroscopy. *Physical Chemistry Chemical Physics* 2009;11:5628-33.
- [37] Bakthavatchalam B, Habib K, Saidur R, Shahabuddin S, Saha BB. Influence of solvents on the enhancement of thermophysical properties and stability of multi-walled carbon nanotubes nanofluid. *Nanotechnology* 2020;31:235402.
- [38] Ghasemi SE, Ranjbar AA, Hosseini MJ. Forced convective heat transfer of nanofluid as a coolant flowing through a heat sink: Experimental and numerical study. *Journal of Molecular Liquids* 2017;248:264-70.
- [39] Nasiri A, Shariaty-Niasar M, Rashidi A, Amrollahi A, Khodafarin R. Effect of dispersion method on thermal conductivity and stability of nanofluid. *Experimental Thermal and Fluid Science* 2011;35:717-23.
- [40] Vajdi M, Sadegh Moghanlou F, Ranjbarpour Niari E, Shahedi Asl M, Shokouhimehr M. Heat transfer and pressure drop in a ZrB<sub>2</sub> microchannel heat sink: A numerical approach. *Ceramics International* 2020;46:1730-5.
- [41] Jia YT, Xia GD, Zong LX, Ma DD, Tang YX. A comparative study of experimental flow boiling heat transfer and pressure drop characteristics in porous-wall microchannel heat sink. *International Journal of Heat and Mass Transfer* 2018;127:818-33.
- [42] Qu W, Mudawar I. Experimental and numerical study of pressure drop and heat transfer in a single-phase micro-channel heat sink. *International Journal of Heat and Mass Transfer* 2002;45:2549-65.